Expect the unexpected: Four hypotheses to explain unexpected critical zone symmetry in hillslopes with opposing aspect

A.M. Donaldson[1], M. Zimmer[1], M.-H. Huang[2], K. Johnson[1,3], B. Hudson-Rasmussen[2], N.Finnegan[1], N. Barling[1], R. Callahan[1]

[1]Department of Earth and Planetary Sciences, University of California, Santa Cruz, CA, USA

[2]Department of Geology, University of Maryland, College Park, MD, USA

[3]Department of Integrative Biology, University of California, Berkeley, CA, USA

Corresponding author: Amanda Marie Donaldson (amdonald@ucsc.edu)

Key Points:

- Aspect-dependent microclimatic and vegetative differences do not correspond to similar physical structure between slope-aspects.
- A more comprehensive understanding of CZ development requires the inclusion of biotic processes.
- Past critical zone weathering processes shape the structure and function of the modern critical zone.

Keywords: microclimate, slope-aspect, saprolite, weathering, topography, biotic

Abstract

The structure of the critical zone is a product of feedbacks between hydrologic, climatic, biotic, and chemical processes. Ample research within snow-dominated systems has shown that aspect-dependent solar radiation inputs can produce striking differences in vegetation composition, topography, and soil depth between opposing hillslopes. However, more research is needed to understand the role of microclimates on critical zone development within rain-dominated systems, especially below the soil and into weathered bedrock. To address this need, we characterized the critical zone of a north-facing and south-facing slope within a first-order headwater catchment located in central coastal California. We combined terrain analysis of vegetation distribution and topography with field-based soil pit characterization, geophysical surveys and hydrologic measurements between slope-aspects. We observed thicker soil profiles, higher shallow soil moisture, and denser vegetation on north facing slopes, which matched previously documented observations in snow-dominated sites. However, average topographic gradient and saprolite thickness were uniform across our study hillslopes, which did not match common observations from the literature. These results suggest dominant processes for critical zone evolution are not necessarily transferable across regions. Thus, there is a continued need to expand critical zone research, especially in rain-dominated systems. Here, we present four non-exclusive, hypotheses of mechanisms that may explain these unexpected similarities in slope and saprolite thickness between hillslopes with opposing aspects. Specifically, we propose both past and present ecohydrologic processes must be taken into account to understand what shaped the present day critical zone.

Plain Language Summary

Small differences in solar radiation and water availability between hillslopes facing opposite directions may lead to distinct vegetation and hillslope structures. However, more research is needed to understand the controls and extent of structural differences in the subsurface, especially in rain-dominated landscapes. To investigate the physical and ecohydrologic characteristics between hillslopes that face opposite directions, we combined terrain analysis, soil pit characterization, geophysical surveys and hydrologic measurements taken from two hillslopes facing opposite directions. We found that the hillslope that faced north had higher oak tree density, deeper soil and higher soil moisture than the hillslope that faced south. These observations match other published studies from a range of landscapes and climates in the northern hemisphere. However, contrary to expectations based on other studies, we found that the slope and weathered bedrock thickness were similar between the two hillslopes. Similarities in deep soil water and increased groundwater response on the hillslope that faces south suggest that how water moves within the hillslope and what water is available to plants may alter how rock breaks down. In addition, historic solar radiation and water availability may be important to understand the present-day hillslope structure.

1 Introduction

The diversity of landforms on Earth’s surface is intrinsically linked to the spatial distribution of the major components of climate: precipitation and air temperature (Perron, 2017; Sharp, 1982). Studies of the development of the critical zone (CZ), which extends from the tops of vegetation to fresh bedrock, investigate the feedbacks between climatic conditions, hydrologic and ecological processes, underlying geology and tectonic stresses at time scales from individual precipitation events (So´lyom and Tucker, 2004) to millions of years (Maher and Navarre-Sitchler, 2019). Differences in subsurface CZ structure (e.g. permeability, porosity, thickness) have been attributed to climate (Anderson et al., 2013; Anderson et al., 2019), underlying lithology (Buss et al., 2017; Hahm et al., 2019; Ma et al., 2021), subsurface water movement (Lebedeva et al., 2014; Rempe and Dietrich, 2014; Lebedeva et al., 2018) and regional tectonics (Moon et al., 2017; Riebe et al., 2001; St. Clair et al., 2015). However, the ability to identify the above and belowground causal mechanisms on CZ development and function across diverse landscapes is currently lacking. A better understanding of the relationship between climate and CZ development is essential to disentangle dominant drivers, improve process-based Earth Systems models (Fan et al., 2019), predict environmental responses to climate change (Ferdowsi et al., 2021; Maxwell and Shobe, 2022), and manage water resources (Fan et al., 2019).

Hillslopes with opposing aspects, or facing opposite directions, provide natural experiments to investigate how small-scale climatic differences control CZ development (Anderson et al., 2014; Chorover et al., 2011). For example, in the northern hemisphere, higher solar radiation inputs on south-facing slopes (SFS) generate hotter and drier conditions compared to north-facing slopes (NFS), which receive less solar radiation per unit area (Pelletier et al., 2017; Yetemen et al., 2015; Poulus et al., 2012). NFS remain cooler and wetter, which promotes the establishment of mesic species and denser vegetation structure (Armesto et al., 1978; Desta et al., 2004; Zapata-Rios et al., 2016). These aspect-dependent differences in vegetation have been invoked as a key factor contributing to physical CZ aspect-dependent asymmetries in water-limited ecosystems (Pelletier et al., 2017; Smith and Bookhagen, 2021).

Researchers have used these small spatial scale differences in solar radiation and vegetation to develop a set of common expectations of aspect-dependent hillslope-scale CZ characteristics (Pelletier et al., 2017; Regmi, McDonald, and Rasmussen, 2019). Specifically, a common expectation is that lower vegetation densities on SFS will reduce soil surface infiltration capacity, enhancing surface runoff and the promotion of sediment transport (Gutierrez-Jurado et al., 2007; Yetemen et al., 2015). Thereby resulting in less steep slopes compared to densely vegetated NFS with less sediment transport efficiency(Inbar et al., 2018; Istanbulluoglu et al., 2008). That said, this is not universally true; case studies have shown colluvial sediment transport processes (e.g. animal burrowing and floral-bioturbation) may dominate over in soil mantled hillslopes (Roering, 2002; McGuire et al., 2014). In these places, hillslope asymmetry may deviate from our current expectations (Pelletier et al., 2017). For example, colluvial sediment transport can increase with vegetation density (Hughes et al., 2009; McGuire et al., 2014), which may enhance erosion on NFS and make them less steep than SFS. Therefore, despite the expectation that SFS will be less steep than NFS, competition exists between sediment transport processes across landscapes, making universal expectations challenging.

Another common expectation is that aspect-dependent differences in vegetation contribute to differences in hydrologic flowpaths and thus the degree of subsurface chemical weathering (Chorover et al., 2011). Specifically, more vegetation on NFS can increase organic matter and contribute to finer soil texture, which increases soil water retention capacity and promotes soil development (Gutierrez-Jurado et al., 2006; Anderson et al., 2014). Below the soil, higher soil water content allows for deeper recharge into the saprolite, which contributes to thicker, more weathered saprolite on NFS (Garcia-Gamero et al., 2021; Langston et al., 2015). However, these expectations are largely based on snow-dominated catchments where other processes, such as freeze-thaw cycles and snowmelt, can compound the role of vegetation across aspect (Befus et al., 2011; Anderson et al., 2013; West et al., 2019; Nielsen et al., 2021). Therefore, despite the expectation that NFS will have a deeper subsurface CZ, this common expectation must be tested in rain-dominated catchments to confirm its transferability across landscapes.

Recent aspect-based studies in rain-dominated catchments have suggested that the role of microclimates on CZ structure is more complex than previously documented in snow-dominated studies (Inbar et al., 2018; Kumari et al., 2020). Hudson-Rasmussen et al. (in-review) combined seismic refraction geophysical surveys with geochemistry data from Pedrazas et al. (2021) to investigate subsurface weathering between opposing slopes within a rain-dominated oak woodland underlain by sedimentary rocks. While they observed slope-aspect differences in vegetation, hillslope steepness, and soil depth, there were not clear aspect-dependent differences in saprolite thicknesses. They suggested that the observed symmetry in saprolite thickness is a relic of past wetter climatic conditions and additional time is required to produce saprolite asymmetry.

Here, we test the current expectation that NFS are wetter, steeper, and have thicker soil and saprolite compared to SFS within a rain-dominated catchment underlain by sedimentary rocks. To do so, we identified a sedimentary catchment with end-member vegetation assemblages (i.e. grasses versus trees) in the central California Coast Ranges and coupled topographic, hydrologic, pedologic, and geophysical data from two adjacent hillslopes with opposing aspects. Based on our observations, we introduce four testable hypotheses that represent exciting frontiers within the ecohydrologic and CZ science communities.

2 Site Description

The study site is a small (0.04 km^2) headwater catchment with an ephemeral stream that drains to the west, referred to as “Arbor Creek” (37”23’36” N, 121”43’ 25” W) within the North Dark Canyon Watershed (0.77 km^2). Arbor Creek Catchment is located within the University of California Blue Oak Ranch Reserve (BORR; Figure 1) from 720 to 790 m above sea level. This reserve is located within the Mt. Diablo Range, ~24 km northeast of San Jose, California, USA.

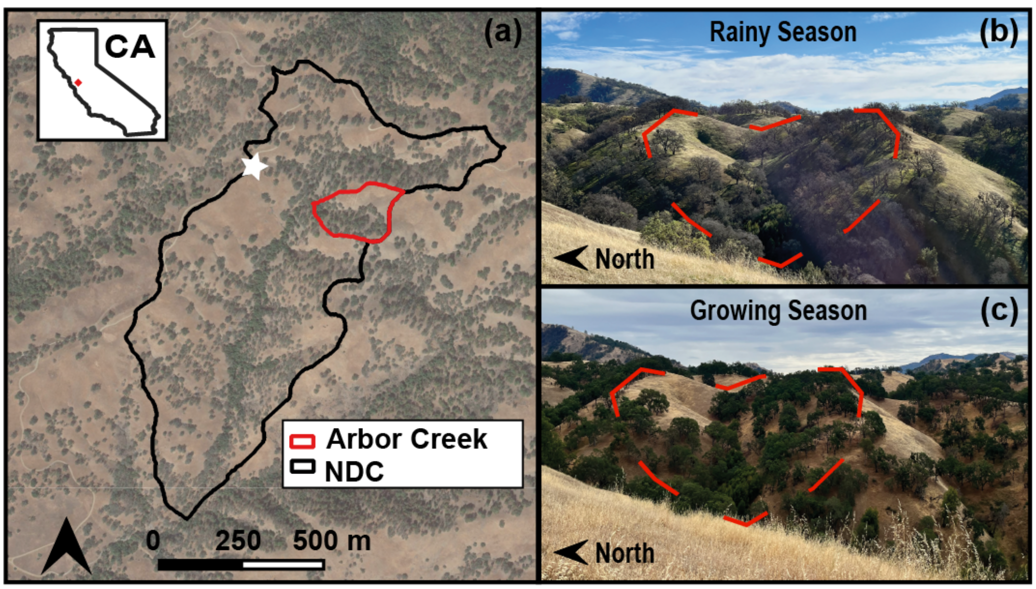

Figure 1. (a) Arbor Creek Catchment area delineated (red) within the larger North Dark Canyon Catchment (NDC, black) and inset map of California, (b) Arbor Creek Catchment during the rainy season (February 2022) and (c) Arbor Creek Catchment during the growing season (June 2022). White star in panel (a) indicates where the rainy season and growing seasons photos of Arbor Creek were taken.

2.1 Geologic and Tectonic Setting

The overall geologic setting of the study site is responding to active geologic processes such as uplift, faulting and landslides (Page, 1999). The study site has no recorded Pleistocene glaciation or peri-glaciation (Marshall et al., 2021). The underlying geology of the Diablo Range has been mapped differently depending on the scale and purpose of investigation from local lithotectonic units observable in an outcrop (Raymond, 2014) to regional tectonic, deformation, and accretion studies that prefer to use the Berkland et al. (1972) belt terminology (Bolhar and Ring, 2001; Ernst, 2011; Raymond, 2018). At the highest resolution of geologic mapping of 1:24,000, Dibblee et al. (2005) characterized the area as Franciscan Assemblage comprised of massive to bedded metagraywacke sandstone, moderately to pervasively sheared shale and melange units (Crawford, 1975), bedded chert, greenstone, and blueschist. In its most general form, the surrounding region has been mapped broadly as “Franciscan complex undifferentiated”, Great Valley Sequence, and the controversial extension of the Eastern Belt/Yolla Bolly Unit with major rock types described as semi-schistose metawacke, meta-mudrock, metachert, and metabasite (Raymond et al., 2018; Wentworth, 1999). Our observations from outcrops within the study site suggest that locally, the dominant rock types are sequences of metagraywacke sandstone, shale, slatey shale with no evidence of chert, blueschist, or melanges, which is best described by the characteristics of the Yolla Bolly Unit and the Great Valley Sequence.

2.2 Climate and Vegetation

Blue Oak Ranch Reserve has a Mediterranean climate characterized by cool, wet winters and warm, dry summers. The average annual rainfall is 600 mm (std dev 200 mm) from 2012 to 2021 and average air temperature of 8°C in January and 25°C in August (http://www.wrcc.dri.edu/weather/ucbo.html). Nearly all precipitation falls as rain between November and April, and the oak tree growing season extends from April to November.

This study area is characterized as a mixed oak savanna-woodland, where vegetation composition throughout the reserve is generally aspect-dependent (Figure 1). Within Arbor Creek catchment, the NFS is a deciduous oak woodland dominated by blue oak (*Quercus douglasii*) and California black oak (*Quercus kelloggii*), with California bay laurel (*Umbellularia californica*) and California buckeye (*Aesculus californica*) present in the lower riparian area. The SFS is predominantly a perennial grassland (*i.e. Bromus diandrus* and *Elymus glaucus*) with sparse blue oak present at lower portions in the catchment that have a southeast slope angle.

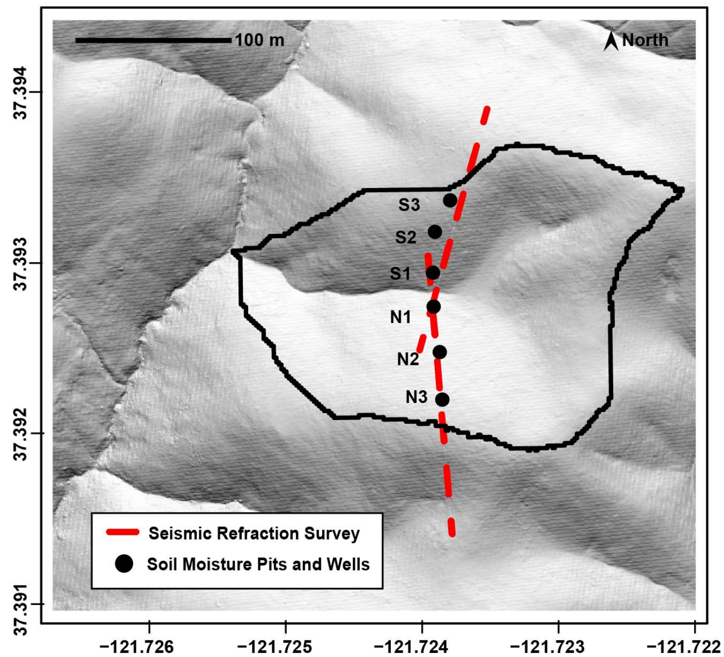

Figure 2. Hillshade of Arbor Creek Catchment showing instrumentation stations with location of soil moisture sensors, groundwater wells (black circles; S3, S2, S1, N1, N2, N3) and seismic refraction transects (red dashed lines).

3 Methods

The principal study transect within Arbor Creek Catchment covers two hillslopes, one NFS and one SFS, that drain to the ephemeral stream channel. On the transect, we established six instrumented stations across different landscape positions: near-stream, mid-slope, and near-ridge; Figure 2).

3.1 Terrain Analysis

We explored relationships between insolation, hillslope gradient, and vegetation using 1-meter resolution 2020 lidar data collected for Santa Clara County (U.S. Geological Survey 2020). We downloaded a bare-earth raster model of these data produced by the USGS, and a raster of unfiltered first-return (vegetation top) data, both from opentopography.org. The first-return data were reprojected and resampled to align with the bare-earth data. Vegetation height was calculated by subtracting the bare-earth data from the first-return (vegetation top) data. A binary tree/no tree layer was generated with a 2 m vegetation height threshold after experimenting and spot checking this threshold against field knowledge. Chaparral is not very common in these areas, but where present is included in the “no tree” category. Insolation was modeled for the bare-earth data in ArcGIS Desktop using the Area Solar Radiation tool as direct radiation, diffuse radiation, and duration of radiation for the solstices, equinox, and annual totals. In addition, slope, aspect, and degrees from south were calculated from the bare-earth data. We compared the distributions of these terrain features in Arbor Creek Catchment to other watersheds in the same local region of the Diablo Range with similar lithology and geomorphic context to assess if the terrain features observed at our study site were representative of the larger region. We excluded infilled and fault-influenced valleys along the San Andreas Fault and excluded areas to the north within the Arroyo Hondo watershed that have much faster incision rates and hence steeper terrain.

3.2 Soil characterization and soil moisture and precipitation measurements

We characterized the soil and top of saprolite at the near-stream, mid-slope, and shoulder positions with soil pits excavated to refusal (~1 m). We delineated soil horizons, depth to saprolite, and characterized parent material within the vertical pit faces. We define the soil as the organic or unconsolidated material that extends from the ground surface to top of the “C” horizon. To quantify variations in shallow and deep soil volumetric water content we installed soil moisture probes (EC-5; METER Group, Inc.; Pullman, Washington) at 10 cm and 50 cm depths below ground, which represented the upper and lower boundary of the soil profile. The measurement accuracy of the EC5 soil moisture sensor is ± 2.5% (Kanso et al., 2020). At the ridge of the NFS, we installed a weather station (ClimaVUE50, Campbell Scientific; Logan, Utah) to record precipitation inputs. We recorded soil volumetric water content (VWC) and precipitation at 10-min intervals from October 1, 2020 to September 30, 2021 (2021 water year).

To characterize seasonal VWC patterns between the NFS and SFS, we separated the VWC time series by the rainy season (October 1, 2020 to March 30, 2021) and the growing season (April 1, 2021 to September 30, 2021). For each season, we calculated the maximum, minimum and average soil VWC. We then compared the difference between maximum, minimum and average VWC between slope-aspect and across landscape position. Lastly, to determine seasonal differences in soil VWC depletion, we characterized the slope of the dry down for each sensor between each event and at the end of the rainy season.

3.3 Saprolite lithology and groundwater measurements

Adjacent to soil pits, we hand-augered 2-inch boreholes to refusal (~1 m) and then drilled with a gas powered backpack drill (Shaw Tool Ltd., Yamhill, Oregon) to 3-5 meters, constrained by the drill's ability to advance through the material. We characterized exhumed borehole samples by lithology type (i.e., shale vs sandstone). Within each borehole, we installed wells to measure groundwater levels every 10 min using pressure transducers (± 0.1 mm resolution; Solinst, California). We screened the wells from the bottom of the adjacent soil pit (~ 1 m) to the bottom of the borehole to isolate hydrologic responses between the soil and underlying saprolite. We quantified the duration of groundwater response for each well as the percent of time that groundwater was present (i.e., sensor readings were >= 0.1 m) from January 27, 2021 to April 26, 2021. This date range presents the period from when all water level sensors were installed to the date of the last rain event for that water year.

3.4 Seismic Refraction

In August 2021, we conducted an active source seismic refraction campaign to investigate subsurface weathering patterns within the CZ. We completed seven surveys along the study transect, with four on the NFS and three on the SFS. We used 48-channel Geode seismographs (Geometrics; San Jose, California). We generated the seismic source by swinging a sledgehammer onto an aluminum plate with 2 to 8 stacked shots adjacent to the survey lines. For the surveys, we used geophone spacing that ranged from 1 to 4 m and shot intervals that ranged from 1 to 8 m (Table 1). It should be noted that the seismic refraction surveys can not be used to determine soil depth because the soil depth is shallower than the vertical resolution of the seismic refraction surveys. We determined the topographic geometry for the seismic model from a 1.5 m spatial resolution DEM collected from an airborne LiDAR mission in 2006.

For each survey, we used the software *Pickwin* (Geometric Inc.) to pick the first P-wave (primary wave from the active seismic source) arrival time to each geophone location. We then performed a Transdimensional, Hierarchical, Bayesian inversion approach with reverse-jump Markov Chain Monte Carlo from Huang et al. (2021). The initial velocity model is proposed by an interpolation of 40 model cells that are randomly distributed in the model domain, and the velocity is ranged from 300 m/s at the surface to 5000 m/s at the bottom of the model. We randomly iterate the velocity model by randomly to create, delete, or move a model cell. We also allow a random model cell to vary its velocity within the range of 300 and 5000 m/s. As the measurement uncertainty is not known, it is inferred by the noise hyperparameter. The THB rjMCMC method randomly accepts or rejects the proposed model based on the algorithm proposed by Metropolis et al. (1953). This method calculates a mean model distribution from an ensemble of posterior velocity models after burn-in that can fit the measured P-wave travel time equally well. With this approach, we can reliably estimate measurement uncertainty as well as model resolving power at depth. After ~6×10^5 iterations of this inversion approach, we used the estimated mean velocity of the ensemble posterior distribution to create a two-dimensional cross section of the best-fit subsurface seismic velocity structure. The interpreted transitional depths in subsurface structure are an approximation due to model structure and limitations (i.e. ray path coverage, smoothing factors, and cell size), but combined with ground-truthed observations of boreholes excavated materials provide a useful approach to identify seismically significant shifts in CZ structure. For more details on post-processing of the seismic velocity model, refer to Huang et al. (2021).

From our resulting velocity models described above, we calculated the vertical velocity gradient, defined as the change of P-wave seismic velocities with depth. Maxima in vertical velocity gradients have been shown to correlate with a transition from highly disaggregated or weathered material to more pristine, low porosity bedrock (Flinchum et al., 2022). Thus, we used vertical velocity gradient profiles across our study transect to identify potential transitions in CZ structure (i.e. porosity and lithology). We calculated the thickness of the saprolite along the survey transect by subtracting the land surface elevations from the average depth of the highest vertical velocity gradient and the corresponding seismic velocity contour, which has previously been shown to represent a transition to saprolite (Flinchum et al., 2018; Hudson Rasmussen et al. in-review). We then binned the data into 5 meter intervals (resolution of seismic data) and compared the difference in the calculated saprolite thickness between the max velocity gradient method and corresponding contour method between hillslope-aspect. We used a Shapiro-Wilk Normality Test to test for normality across the different datasets. We determined whether the differences between slope-aspects across landscape positions are statistically significant using t-tests for parametric data and the Mann-Whitney U tests for non-parametric data (McKnight and Najab, 2010).

Table 2. Geometric information for the seven seismic refraction surveys.

Line Number	Line name	Date collected	Geophone spacing (m)	Shot spacing (m)	Stack #	Seismic line length (m)
1	SFS_deep	10 August 2022	3	8	8	144
2	SFS_shallow 1	10 August 2022	1	1	2	48
3	SFS_shallow 2	10 August 2022	1	1	2	48
4	NFS_deep	11 August 2022	4	8	8	192
5	NFS_shallow 1	11 August 2022	1	1	2	48
6	NFS_shallow 2	11 August 2022	1	1	2	48
7	NFS_shallow 3	11 August 2022	1	1	2	48

3 Results

3.1 Terrain characteristics

Insolation has the greatest influence on tree presence in our study area (Supplementary Figure 1, dashed line). Above about 2500 WH/m^2, we see a decrease in the ratio of hillslope pixels classified as trees (Supplementary Figure 1, dashed line). This pattern can be observed qualitatively on the landscape most readily when looking at the contrast between adjacent NFS and SFS, which average around 1500 WH/m^2 (~60% tree pixels) and 3500 WH/m^2 (~20% tree pixels) respectively in this local region (e.g. Figure 2, Supplementary Figure 1). Within Arbor Creek Catchment, hillslope pixels oriented within 45 degrees of N and S have similar distributions of slope angles (mean slope of 23.7° on NFS and 24.4° on SFS) (Figure 3a). Despite variability in hillslope orientation due to stream network shape, when comparing pixels across the larger region, NFS and SFS also have similar slope angle distributions e (24.7 on NFS and 23.2 on SFS).

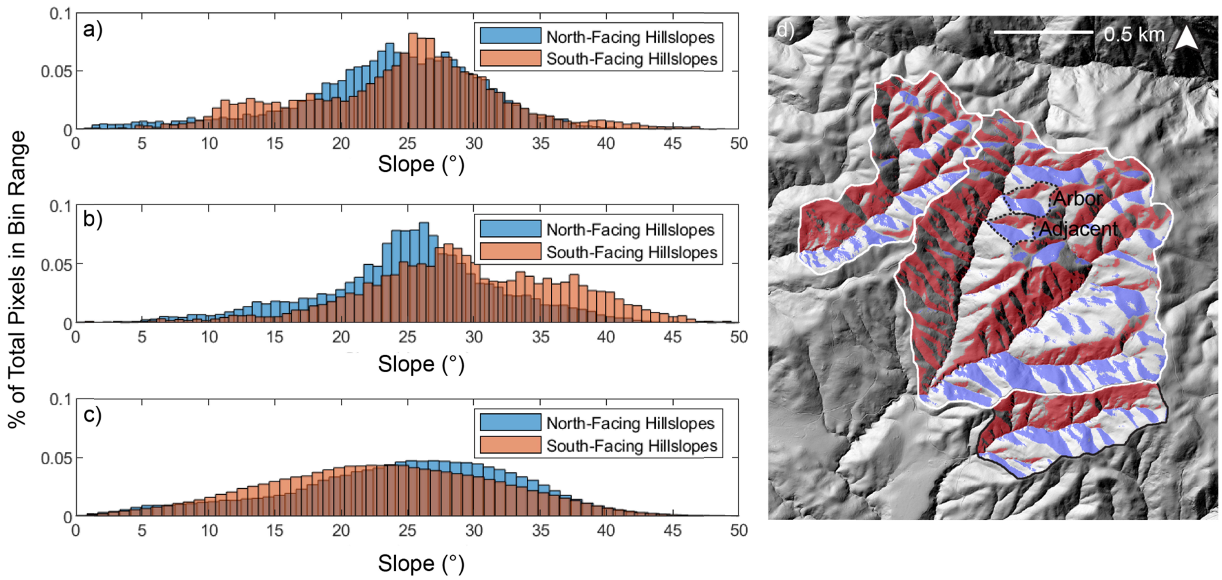

Figure 3. Slope distributions (a) for Arbor Catchment (delineated in black (d)), for an (b) adjacent catchment to the south with similar solar orientation (delineated in black (d)), and for a (c) broader sample of catchments in the local region with similar geomorphology and lithology (delineated in white (d)).

3.2 Soil characteristics

Across the six soil pits, the soil depth ranged from 30 to 80 cm, with a mean depth of 51 cm (Supplementary Table 1). On the NFS, soil depth varied by landscape position, with the shallowest soil depth occurring at the near-stream position (30 cm), the deepest soil depth at the mid-slope (80 cm) and intermediate depth (50 cm) at the near-ridge position. On the SFS, the soil depth was more uniform relative to the NFS, the near-stream and mid-slope both had 55 cm soil depths while the near-ridge soil depth was only 30 cm (Figure 4).

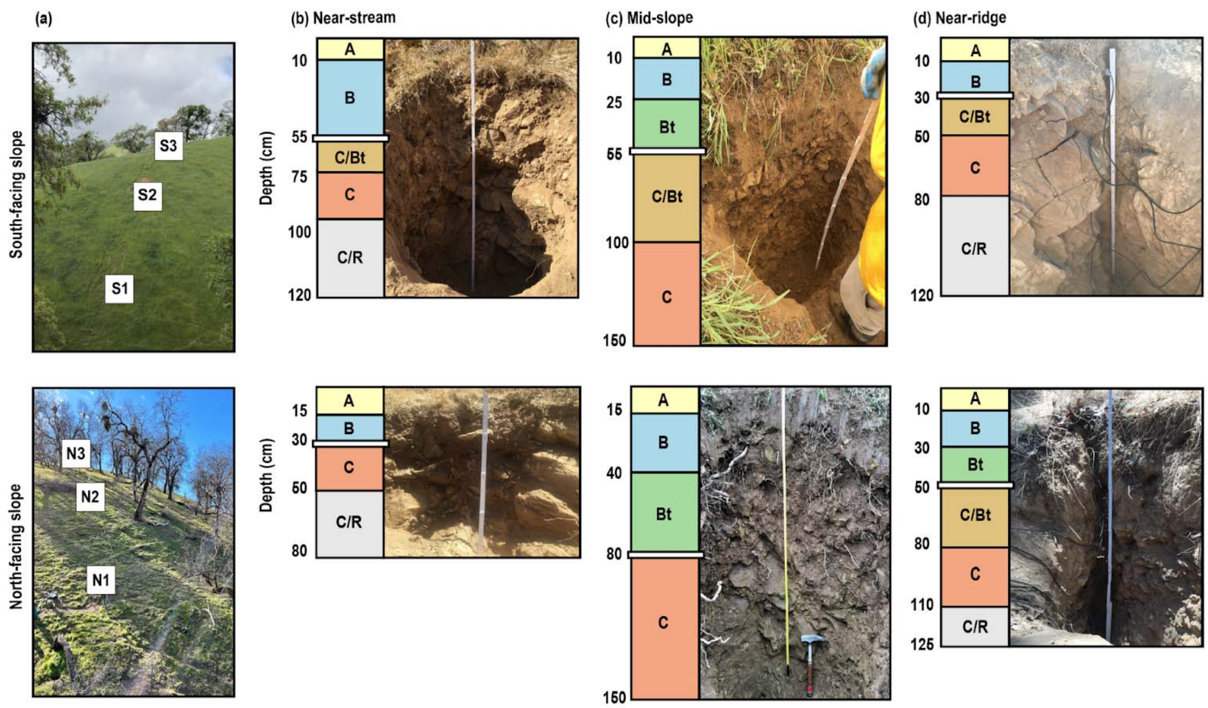

Figure 4. (a) Images of Arbor Creek Catchment's SFS and NFS. Soil pit images with soil horizons delineated at the (b) near-stream, (c) mid-slope and (d) near-ridge landscape positions. White line on the illustrated monolith represents the transition between soil to saprolite.

3.3 Saprolite characteristics

The seismic refraction mean velocity, vertical velocity gradient, and coefficient of variation are shown in Figure 5, showcasing the similarity in saprolite thickness between slope-aspects. The max vertical velocity gradient best corresponds to depth at which the seismic velocity ranges from 1200 m/s to 1400 m/s (Supplementary Figure 3). This range is similar to velocities used to distinguish the saprolite-weathered bedrock transition in sandstones and mudstones (1300 m/s; Hudson Rasmussen et al., in-review) and granitic gneiss (1400 m/s; Flinchum et al., 2019). We therefore inferred that the transition between the saprolite and weathered bedrock occurred within the range of the max velocity gradient, the depth to the 1200 m/s and 1400 m/s seismic velocity contour. We observed the thickness of the saprolite to generally decrease from the ridge to the stream channel (Figure 6). These geophysical observations indicate that the saprolite thickness is similar between hillslopes with opposing aspects (Figure 6). Though the maximum vertical velocity gradient is systematically higher on the NFS (686 m/s/m) compared to the SFS (277 m/s/m). Based on the depth to the maximum gradient, the average saprolite depth was 6.6 ± 0.31 m and 5.7 ± 0.32 m on the NFS and SFS, respectively, and not statistically significant between slope-aspects ($t = 1.89$ p-value = 0.07). Based on the depth to the 1200 m/s contour, the average saprolite depth was 6.1 ± 0.42 m and 5.6 ± 0.27 m for the NFS and SFS, respectively, which were not statistically different ($t = 0.95$, p-value = 0.34). Finally, using the 1400 m/s velocity contour, the saprolite depth, 7.5 ± 0.64 m and 7.3 ± 0.49 m for the NFS and SFS respectively, was also not statistically different ($W = 145.5$, p-value = 0.72).

Below the maximum vertical velocity gradient, the seismic velocity increased from ~1300 m/s to 3000 m/s on average in 26 m from the surface (std 10 m) and 49 m (std 11 m) on the SFS and NFS, respectively. The increase in the seismic velocity could be due to a gradually decreasing porosity (Figure 5; Gu et al., 2020; Flinchum et al., 2022). This transition most likely represents the transition from weathered bedrock (more competent than the saprolite above) to more pristine, low porosity material. The P-wave velocity of pristine (not chemically altered) sandstone with < 20% porosity has been shown to be > 3800 m/s (Geldart & Sheriff, 2004). However, due to the low seismic refraction resolution at depth we can not reliably provide insight into the transition between weathered to fresh bedrock. In addition, based solely on the seismic velocity data, we are unable to distinguish between weathered bedrock with low fracture density or fresh bedrock with high fracture density.

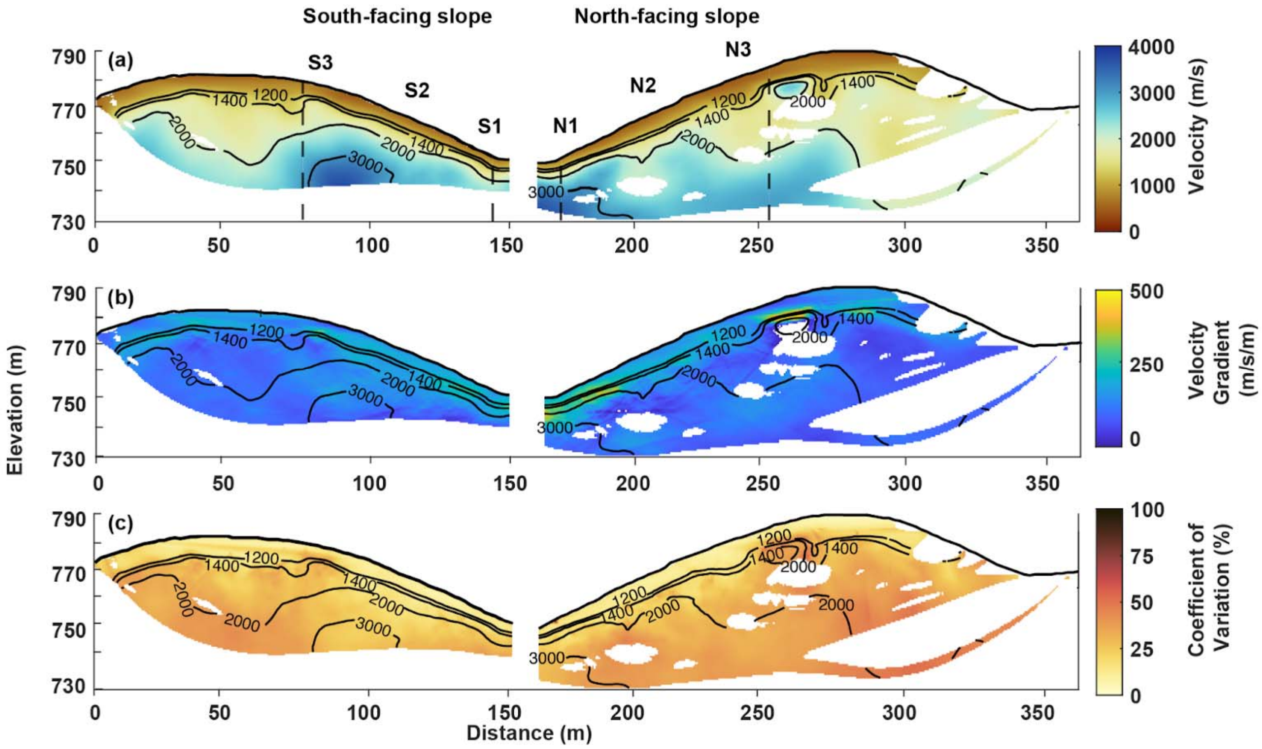

Figure 5. (a) Mean seismic refraction velocity model, (b) mean vertical velocity gradient, and (c) coefficient of variation for velocity model (inferred as model uncertainty) with 1200 m/s, 1400 m/s, 2000 m/s, and 3000 m/s velocity contours. Dashed lines in panel (a) represent the hillslope length further analyzed for saprolite thickness.

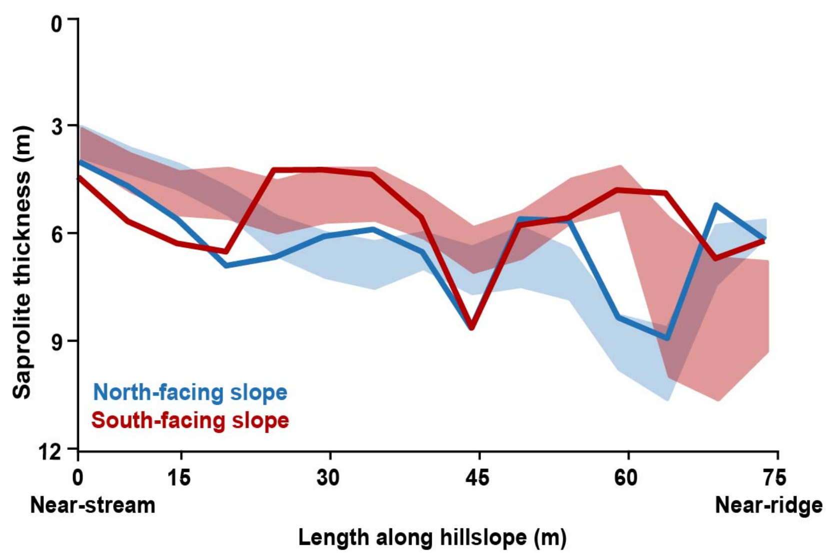

Figure 6. Average saprolite depth based on the depth to the 1200 m/s velocity contour and 1400 m/s velocity contour (top and bottom of shaded region, respectively) and the max velocity gradient (bold lines) for the NFS (blue) and SFS (red) across the study hillslope.

3.4 Soil moisture and groundwater responses

During the rainy season, the maximum soil VWC at the 10 cm depth was similar between the NFS and SFS at the near-stream and near-ridge positions, but was higher on the NFS at the mid-slope position. The average difference between the maximum VWC on the NFS and SFS at the 10 cm depth was 4%, 9% and 1% at the near-stream, mid-slope and near-ridge, respectively. At the 50 cm depth the average difference between the max VWC on the NFS and SFS was 3%, 6% and -1% at the near-stream, mid-slope and near-ridge, respectively.

Between rain events at the 10 cm depth the SFS dried down more than the NFS (Figure 7) across all landscape positions. However, between rain events at the 50 cm depth the NFS and SFS dried down similarly at the near-stream and mid-slope position (Figure 7). In addition, while there were aspect-dependent differences in dry down characteristics during the growing season, the NFS and SFS dried down to similar VWC. Specifically, during the beginning of the growing season in 2021 (April - May), the soil VWC was higher on the NFS compared to the SFS except at the midslope position where the soil VWC was similar at the 50 cm depth (Figure 7). From April to May, the SFS dried down more than the NFS across all landscape positions and depths. By July, the NFS and the SFS soil dried down to similar and constant VWC at the 10 cm depth. However, at the 50 cm depth, the SFS had dried down to a relatively constant VWC in June while the NFS continued to dry down until September. At the end of the growing season (October), the soil VWC was similar between slope-aspects across all landscape positions except at the midslope position where the NFS was 9% drier than the SFS.

Observed water levels in boreholes indicated higher groundwater storage on SFS compared to NFS at the mid-slope and near-ridge landscape positions (Figure 8).

During the period of observation for groundwater (January 27 2021 - April 28 2022), water levels responded to incoming precipitation events across all landscape positions on the SFS, but only responded at the near-stream position on the NFS. Here, the dominant lithology is shale, which differs from the other sandstone-dominated landscape positions. On the NFS, groundwater was measurable 99%, 0% and 0% of the observation period for the near-stream, mid-slope, and near-ridge positions, respectively. On the SFS, groundwater was measurable 21%, 98% and 2% for the near-stream, mid-slope, and near-ridge positions, respectively. While the groundwater level at the SFS mid-slope was sustained throughout the observation period, groundwater levels at the near-stream and near-ridge position were transient and only responded to precipitation events.

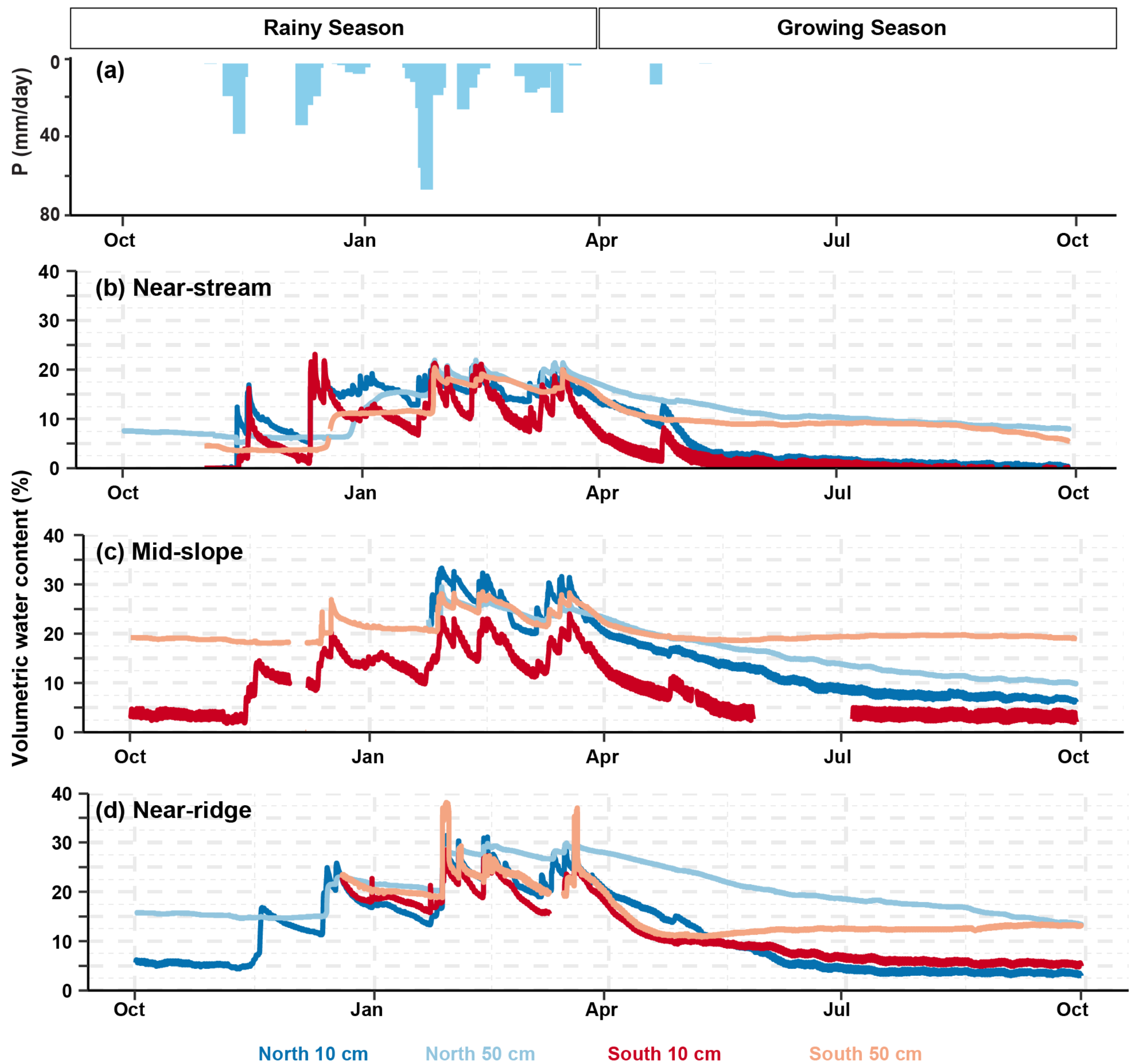

Figure 7. (a) Precipitation time series; Soil volumetric water content at the (b) near-stream, (c) mid-slope, and (d) near-ridge landscape positions. At each landscape position, 10 cm (light) and 50 cm (dark) depths are shown for NFS (blues) and SFS (reds). Missing data are due to sensor malfunction.

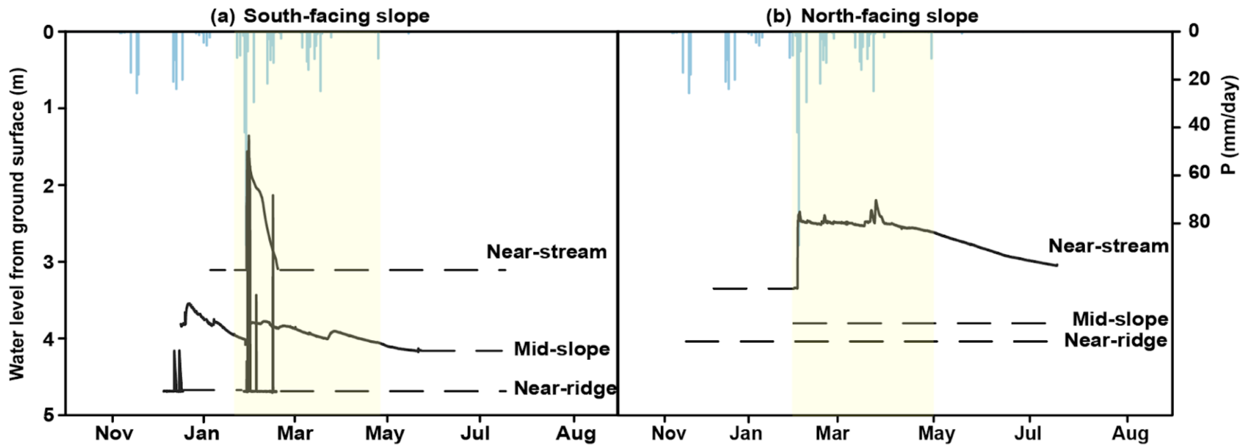

Figure 8. (a) SFS water table elevation and (b) NFS water table elevation during the 2021 water year for the near stream, mid-slope and near-ridge landscape positions. Missing data at the beginning of the water year are due to delayed sensor installation and dashed lines represent no water present at the bottom of the well. The yellow shaded region indicates the time period when groundwater duration was quantified (January 27, 2021 - April 28, 2022)

4 Discussion: Testable hypotheses to explain the unexpected symmetry in hillslope steepness and saprolite thickness between hillslopes with opposing aspects

Here, we discuss how the observed physical and ecohydrologic critical zone characteristics of Arbor Creek Catchment compare to current slope-aspect conceptual models. These existing expectations are borne out of extensive work in snow-dominated landscapes and suggest cooler, densely vegetated NFS will have steeper slopes, higher soil water content, more groundwater recharge and thicker soil and saprolite compared to warmer, sparsely vegetated SFS (Pelletier, 2017). At our site, we observed that NFS had higher vegetation density and shallow soil water content, which is in agreement with current common expectations (Figure 7). However, beyond the shallow soil layer, we observed higher groundwater levels and deep soil moisture on SFS. In addition, between slope-aspects hillslope steepness and saprolite thickness were similar between slope aspects. These observations deviate from current common expectations. We introduce four hypotheses that provide testable, non-exclusive mechanisms that may explain deviations from the current common expectations for slope (Sections 4.1 and 4.4) and saprolite thickness (Sections 4.3, 4.2, 4.4; Figure 9).

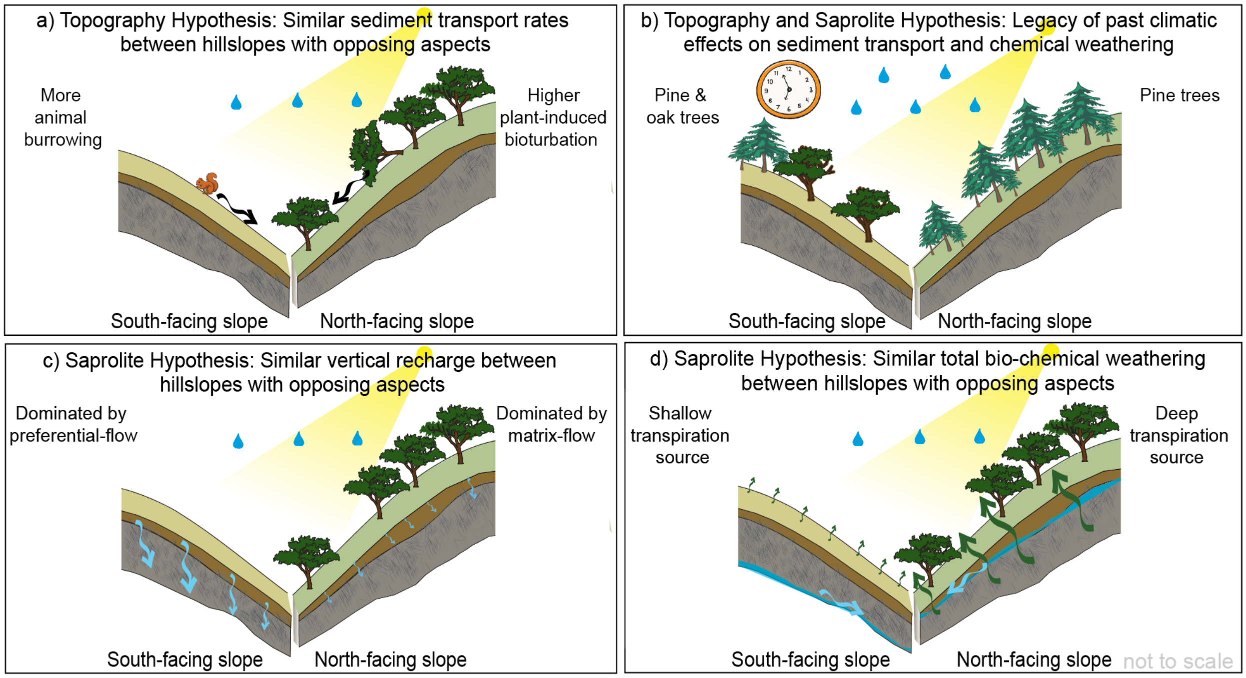

Figure 9. Four hypotheses to explain similar hillslope steepness and saprolite thickness between hillslopes with opposing aspects. a) Similar sediment transport rates despite diverging drivers (animal burrowing on SFS; bioturbation on NFS) , b) Contemporary slope and saprolite thickness still reflects the legacy of past climates, c) Similar vertical recharge driving similar chemical weathering rates at saprolite interface between hillslopes, despite diverging recharge mechanisms (preferential flow on SFS; matrix flow on NFS) and d) Similar total bio-chemical weathering between hillslopes with opposing aspects, despite varying proportions of biological and chemical weathering.

4.1 Topography Hypothesis: Similar hillslope steepness is driven by uniform soil transport rates from aspect-dependent mechanisms

A common expectation is that sparsely vegetated SFS will have higher fluvial sediment transport, resulting in less steep slopes compared to NFS (Gutierrez-Jurado et al., 2007; Inbar et al., 2018; Istanbulluoglu et al., 2008; Yetemen et al., 2015). Within

Arbor Creek Catchment and the larger BORR area, we observed similar hillslope steepness between the NFS and SFS (Figure 3). Importantly, we do not see evidence for fluvial sediment transport (e.g. rills and gullies) throughout BORR, suggesting that colluvial sediment transport may be more dominant. We propose that the observed topographic symmetry between hillslopes with opposing aspects may be explained by a balance between distinct dominant colluvial sediment transport processes on hillslopes with opposing aspects (Figure 9a). Specifically, we propose that the balance between root-induced hillslope stabilization and sediment transport via wind-thrown trees may contribute to a net downslope sediment flux equivalent to the higher sediment transported on SFS from animal burrowing.

Small mammal burrowing is potentially a significant mode of sediment transport in steeply sloped and soil mantled hillslopes (Black and Montgomery, 1991; Gabet et al, 2003). Although knowledge on the role of animal burrowing on sediment transport is limited to few species and ecoregions, previous studies have identified a relationship between animal burrows and incoming solar radiation (Hall and Lamont, 2003; Übernickel et al., 2021). For example, Übernickel et al. (2021) conducted an inventory of burrowing animal entrances between NFS and SFS across four study sites with a hydroclimatic gradient in Chile. Their inventory revealed that the majority of small-animal entrances were located on the NFS. Within the Southern Hemisphere, NFS receive higher amounts of solar radiation compared to SFS (Poulus et al., 2012).They hypothesized that although more food and shelter may be present on the densely vegetation SFS, warmer temperatures on the NFS during the winter months may be favorable habitat for burrowing animals long-term.

Increased woody vegetation on a landscape can have important implications for sediment transport due to higher rates of floral-induced bioturbation (e.g. root-decay, and wind-throw) (Gabet and Mudd, 2010). For example, Hughes et al. (2009) suggest that a successional vegetation shift from a grass-shrub land to a forested landscape led to a significant increase in floral-induced sediment transport due to wind-throw. While little research exists to the authors knowledge on the causes, effects, and prevalence of windthrow in oak woodlands, there are several studies investigating the effects of forest regeneration after wind disturbance in mixed-deciduous forest including oaks (Götmark and Kiffer 2014, Szwagrzyk et al., 2018). These studies suggest that windthrow may be an important component of forested disturbance regimes (Cannon et al., 2017), which has unknown consequences for sediment transport. Therefore, more research is needed to have a better understanding of the potential for wind-throw to promote sediment transport on tree-dominated NFS, compared to grass-dominated SFS.

Within the context of our study site, these findings suggest that within Arbor Creek Catchment, prevalent animal burrowing on the warmer SFS may contribute to equivalent sediment transport downslope by bioturbation (e.g. animal burrowing and tree-throw) on the NFS over long-term timescales. Future research to test this hypothesis would require a quantification of animal burrowing between hillslopes with opposing aspects (Dixon et al., 2009), an understanding of the prevalence and geomorphic impact of tree-throw within oak woodlands (Doane et al., 2021), and ideally the use of cosmogenic radionuclides as a tool to measure surface erosion rates between hillslopes with opposing aspects over long timescales (Anderson et al., 2021).

4.2 Topography and Saprolite Hypothesis: Legacy of past climatic effects on sediment transport and chemical weathering

An alternative explanation for similar hillslope steepness at our study site may also explain the similar saprolite thickness between hillslopes with opposing aspects. Specifically, despite the expectation that NFS should have steeper slopes and a thicker saprolite compared to SFS, it is possible that the actively eroding landscapes of central coastal California require longer geologic time under the current climatic conditions to produce the expected topographic and subsurface asymmetries, even though sufficient time has passed to produce differences in vegetation and soil depth (Figure 9b). This is supported by previous studies that have demonstrated that delayed geomorphic adjustments to climatic fluctuations can lead to complex observations of soil erosion, soil thickness and topographic gradients (Heismath et al., 1999, Hughes et al., 2009; Hudson-Rasmussen et al., in-review).

The extent that processes in the past (from days to millenia) control contemporary processes varies across ecosystem functions (i.e. runoff, vegetation distribution, rock weathering). For example, timescales relevant to vegetation shifts can range from decades to centuries (Corlett and Westcott, 2013), while rock weathering patterns emerge over millennia to hundreds of millennia (Lebedeva and Brantley, 2020). For example, if we estimate a 0.05-0.10 mm/yr erosion rate in the California Central Coast Ranges (*sensu* Montgomery, 1993), the maximum and minimum time required to develop the observed 5 m thick saprolite is 50,000-100,000 years. Therefore, we can assume that saprolite thickness is not only dictated by the climatic and vegetative conditions during the present-day Holocene, but also the late Pleistocene (2.58 mya to 0.012 mya). Paleoclimatic records from across California suggest that during the Pleistocene, climatic conditions were cooler and wetter, with potentially more intense precipitation events compared to the present-day Holocene (Daniels et al., 2005; Kulongoski et al., 2009).

Climatic shifts can have important implications for vegetation dynamics (Huesser et al., 1998) that can influence soil development and erosion, weathering rates and subsurface water storage (Jackson et al., 2000; Ivory et al., 2014; Hagedorn et al., 2019). The transition from the wetter, cooler Pleistocene to the warmer, drier Holocene contributed to a dramatic shift in dominant vegetation composition across California (Heusser et al., 1998). Pollen analyses from sediment cores and Neotoma (packrat) middens suggest these landscapes were previously dominated by pinus species and that oak woodlands did not become well-established until the early-mid Holocene (Cole, 1983; Byrne et al., 1991; Heusser et al., 1998; Mensing, 2005). Furthermore, Mensing (2005) suggested that if oak trees were present during the late Pleistocene, it was “likely on the warmer SFS.” This suggests that the characteristic grass-dominated SFS and oak-tree dominated NFS we observe today may only be a relatively recent (~10,000 years) phenomenon. Therefore, it is plausible that the legacy of pine and oak trees on the SFS, and the associated weathering impacts (Paulik et al., 2016; Hassenmueller et al., 2022; Tague, 2022), may contribute to the symmetry in hillslope steepness and saprolite thickness between hillslopes with opposing aspects (Figure 9b).

4.3 Saprolite Hypothesis: Similar vertical recharge between hillslopes with opposing aspects despite aspect-dependent flowpaths

A common expectation is that densely vegetated NFS will have higher vertical recharge due to sustained elevated soil moisture and higher infiltration capacity (García-Gamero et al., 2021). This enhanced vertical recharge has been suggested to promote thicker saprolite on NFS than SFS (Langston et al., 2015; Nielson et al., 2021). However, we observed similar soil moisture content at deeper portions of the soil profile, higher occurrence of groundwater response on the SFS compared to the NFS, and similar saprolite thicknesses between slopes. We propose that the uniform weathering required to produce similarities in saprolite thickness across slopes is driven by distinct aspect-dependent hydrologic flowpaths, as evidenced by the deviation in groundwater responses. Specifically, the extent and magnitude of vertical recharge to the saprolite, and thus water available for chemical weathering, are similar due to higher matrix flow on NFS and preferential flow on SFS (Figure 9c).

Most field-based studies that characterize vertical hydrologic flowpaths have been constrained to soil due to the difficulty of monitoring hydrologic flowpaths deeper in the subsurface. That said, these studies have demonstrated that preferential flow can significantly enhance subsurface recharge (Hinkley et al., 2014). For example, Hinkley et al., 2014 used a tracer experiment to characterize the snow-melt water movement timing and magnitude between NFS and SFS within Gordon Gulch (Colorado, USA). They showed that there was a higher occurrence of preferential flow on SFS compared to NFS, which led to more water entering SFS compared to the matrix flow-dominated NFS. They hypothesized that increased preferential flow of SFS was likely due to soil structure (e.g. texture, animal burrows) and/or high water supply via snowmelt that contribute to preferential flow activation even during unsaturated conditions (Nimmo, 2012). In addition to subsurface physical structure and water supply rates, antecedent soil moisture conditions exert a strong control on the occurrence of preferential flowpaths (Tang et al., 2020). Specifically, drier soils on the SFS may promote preferential flowpaths along cracks in clay-rich soil or well-connected saprolite fractures (Nimmo et al., 2021). Despite the demonstrated prevalence of preferential flowpaths, more research is needed to understand how the extent and magnitude of water delivered along preferential flowpaths compares to matrix-dominated flowpaths.

The common expectation that NFS have higher matrix flow and higher subsurface water availability than SFS has important implications for how the CZ community conceptualizes saprolite weathering between slope-aspects. Due to the limited direct-observation of hydrologic flowpaths within the saprolite, most studies investigating the climatic and hydrologic controls on saprolite development have been achieved through numerical modeling. Within Gordon Gulch, Langston et al. (2015) was able to include preferential flow within their model of snow-melt recharge and saprolite weathering between hillslope with opposing aspects. While they were able to demonstrate that preferential flow along fracture planes increased the recharge rate and wetting extent when they were activated, they did not include any aspect-dependent differences in preferential flow occurrences. As expected, the NFS had a thicker saprolite than the SFS due to higher antecedent moisture conditions that led to increased effective hydraulic conductivities. However, the role of distinct dominant hydrologic flowpaths (e.g. matrix flow versus preferential flow) in saprolite weathering remains unclear.

Future research to address this hypothesis would require the characterization of recharge rates and occurrence of preferential flowpaths between slope-aspects within rain-dominated systems. A particular emphasis should be placed on the quantification of hydrologic flow (e.g. residence times and dominant flowpaths) within the saprolite under different precipitation regimes and hydrologic and geologic conditions. Lastly, these field-based methods must be incorporated into a numerical model with variable flow to better constrain the hydrologic controls on saprolite development between hillslopes with opposing aspects.

4.4 Saprolite Hypothesis: Similar total bio-chemical weathering between hillslopes with opposing aspects

An alternative explanation for similar saprolite thickness across hillslopes with opposing aspects is that cumulative weathering of saprolite from both chemical and biological processes is uniform across slopes. Specifically, the degree of chemical weathering on the SFS matches the degree of weathering from both chemical and biological weathering on the NFS. Within Arbor Creek, the SFS had more persistent groundwater at the saprolite-weathered bedrock interface, except at the NFS near-stream position, which is dominated by a different lithology than the rest of the study site (shale instead of sandstone; Figure 8). We hypothesize this groundwater presence enhances lateral flow of chemically equilibrated water and subsequent replacement with non-equilibrated meteoric water on SFS, which accelerates chemical weathering on SFS (Rempe and Dietrich, 2014; Wang et al., 2021). In contrast, lateral flow toward the stream on NFS may be lower due to limited saturated conditions in the saprolite from oak uptake of water during the growing season. At the same time, deeply rooted oak trees on NFS may enhance biologically driven weathering. Therefore, we hypothesize that the NFS's cumulative effects of reduced chemical weathering by limited lateral flow and enhanced biological weathering from vegetation balances the dominating chemical weathering on SFS and may contribute to the observed symmetry in saprolite thickness across slopes.

Lateral flow downgradient can occur when permeability of an overlying layer is greater than one magnitude of the underlying layer (Brantley et al., 2017). This perched, lateral drainage of chemically equilibrated fluids and subsequent replenishment with chemically active fluids is a process that has been proposed to dictate the extent of subsurface chemical weathering (Rempe et al., 2018). As our geophysical results show uniform saprolite thickness across slopes, if this process acted in isolation it would require lateral flow to also be uniform across slopes. However, we observe a higher groundwater response on the SFS compared to the NFS, which suggests that the SFS may have higher occurrences of lateral flow. One possible explanation for symmetry in saprolite thickness between hillslopes with opposing aspects, and not a thicker saprolite on SFS, may be due to the deeply rooted oak trees on NFS.

Several mechanisms allow for plant roots to directly and indirectly promote subsurface weathering processes. For example, strain-induced porosity production due to root-wedging between existing fractures may contribute significantly to subsurface weathering (Hayes et al., 2019). Abiotic chemical weathering is strongly influenced by plant water uptake and redistribution which can alter weathering pathways (Lucas et al., 2001). As deeply rooted oaks utilize water stored within the saprolite for transpiration

(Hahm et al., 2020; 2022), a depletion in water content within the saprolite during the growing season could have consequences for water residence times and solute production in the subsequent rainy season.

5 Conclusion and next steps

Within a rain-dominated landscape underlain by sedimentary rocks, we used a multidisciplinary approach to investigate the influence of microclimates on CZ structure between hillslopes with opposing aspects. We observed that CZ structure between hillslopes with opposing aspects does not fully align with current conceptual models from the literature that are largely based on snow-dominated landscapes underlain by igneous rocks.

We found that on a regional scale, decreased solar radiation correlated with increased tree presence. This aligns with observations within our localized study site, Arbor Creek Catchment, where the cooler NFS was dominated by oak trees while the warmer SFS was dominated by grasses. However, the hillslope steepness and saprolite thickness was similar between hillslopes with opposing aspects, which was counter to expectations. Deep soil moisture measurements indicated that although SFS dry down more rapidly at the soil-saprolite boundary, the maximum water content is similar between opposing aspects. In addition, groundwater measurements suggest that there is increased groundwater stored on the SFS compared to the NFS, which is also contrary to previous slope-aspect hydrologic studies.

We present four testable hypotheses to explain the observed similarity in topographic gradients and saprolite thickness between hillslopes with opposing aspects. Here, we highlight that past and present biotic processes may alter the subsurface hydrologic environment, which has consequences for present-day water cycling and long-term CZ development. Further research exploring these testable hypotheses across rain-dominated systems with different precipitation magnitudes, vegetation types and geologic settings will better constrain the prevalence of these potential mechanisms. In addition, the integration of preferential flowpaths, paleovegetation distributions and plant-driven alterations in hydrologic flowpaths into numerical models is an important frontier in aspect-dependent CZ development. Such research is critically needed to identify the relationship between vegetation, hydrologic flowpaths and chemical weathering, which has important implications for water resources management and ecosystem health within a changing climate.

Acknowledgments

The authors would like to acknowledge the financial support provided by the Betty and Gordon Moore Foundation under the project title: The California Heartbeat Initiative, National Science Foundation CAREER grant (Award #2046957), and the Mildred E. Mathias Graduate Student Research Grant by the University of California Natural Reserve System. In addition, the authors would like to acknowledge the financial support granted by the University of California, Santa Cruz through the Kathryn D. Sullivan Impact Award and the Zhen and Wu Memorial Fund Award. The authors thank past and present members of the Zimmer Watershed Lab, namely, Chris Causbrook, Peter Willits, Michael Wilshire and Lauren Giggy for support in the lab and field. Members of the California Heartbeat Initiative-Freshwater program, Todd Dawson, Jim Norris, and Collin Bode provided thoughtful guidance and key technical assistance throughout the project. In addition the authors would like to thank Zac Harlow and Zac Tuthill for land access and troubleshooting enthusiasm.

Open Research

All data used in the publication are cited in the references and hosted on Consortium of Universities for the Advancement of Hydrologic Science, Inc. (CUAHSI)'s web based hydrologic information system (Hydroshare). Donaldson, A. M. (2022). Expect the unexpected: Four hypotheses to explain unexpected critical zone symmetry in hillslopes with opposing aspect, HydroShare, http://www.hydroshare.org/resource/9a9897aa0bb14d20ab4189b98a8439f6. The THB rj-MCMC software for active source seismic refraction inversion is available in Github (https://github.com/MongHanHuang/THB_rjMCMC) (Huang et al., 2021).

References

Anderson, R. S., Rajaram, H., & Anderson, S. P. (2019), Climate driven coevolution of weathering profiles and hillslope topography generates dramatic differences in critical zone architecture. Hydrological Processes, 33(1), 4–19. https://doi.org/10.1002/hyp.13307

Anderson, R. S., Anderson, S. P., & Tucker, G. E. (2013), Rock damage and regolith transport by frost: an example of climate modulation of the geomorphology of the critical zone. Earth Surface Processes and Landforms, 38(3), 299–316. https://doi.org/10.1002/esp.3330

Anderson, S. P., Kelly, P. J., Hoffman, N., Barnhart, K., Befus, K., & Ouimet, W. (2021). Is This Steady State? Weathering and Critical Zone Architecture in Gordon Gulch, Colorado Front Range. Hydrogeology, Chemical Weathering, and Soil Formation, 231–252. https://doi.org/10.1002/9781119563952.ch13

Anderson, S. P., Hinckley, E.-L., Kelly, P., & Langston, A. (2014), Variation in Critical Zone Processes and Architecture across Slope Aspects. Procedia Earth and Planetary Science, 10, 28–33. https://doi.org/10.1016/j.proeps.2014.08.006

Armesto, J. J., & Martinez, J. A. (1978), Relations Between Vegetation Structure and Slope Aspect in the Mediterranean Region of Chile. Journal of Ecology. Vol. 66, No. 3. pp. 881-889. https://doi.org/10.2307/2259301

Befus, K. M., Sheehan, A. F., Leopold, M., Anderson, S. P., & Anderson, R. S. (2011), Seismic Constraints on Critical Zone Architecture, Boulder Creek Watershed, Front Range, Colorado. Vadose Zone Journal, 10(3), 915. https://doi.org/10.2136/vzj2010.0108

Berkland, J.O., Raymond, L.A., Kramer, J.C., Moores, E.M., and O'Day, M. (1972), What is Franciscan?: American Association of Petroleum Geologists Bulletin, v. 56, p. 2295–2302. https://doi.org/10.1306/819A421A-16C5-11D7-8645000102C1865D

Black, T. A., & Montgomery, D. R. (1991), Sediment transport by burrowing mammals, Marin County, California. Earth Surface Processes and Landforms, 16(2), 163–172. https://doi.org/10.1002/esp.3290160207

Bolhar, R., and Ring, U. (2001), Deformation history of the Yolla Bolly terrane at Leech Lake Mountain, Eastern belt, Franciscan subduction complex, California Coast Ranges. GSA Bulletin 113 (2): 181–195. https://doi.org/10.1130/0016-7606(2001)113<0181:DHOTYB>2.0.CO;2

Brantley, S. L., Lebedeva, M. I., Balashov, V. N., Singha, K., Sullivan, P. L., & Stinchcomb, G. (2017). Toward a conceptual model relating chemical reaction fronts to water flow paths in hills. *Geomorphology*, *277*, 100–117. https://doi.org/10.1016/j.geomorph.2016.09.027

Buss, H. L., Chapela Lara, M., Moore, O. W., Kurtz, A. C., Schulz, M. S., & White, A. F. (2017). Lithological influences on contemporary and long-term regolith weathering at the Luquillo Critical Zone Observatory. Geochimica et Cosmochimica Acta, 196, 224–251. https://doi.org/10.1016/j.gca.2016.09.038

Byrne, R., Edlund, E., & Mensing, S. A. (1991). Holocene changes in the distribution and abundance of oaks in California. USDA Forest Service General Technical Report PSW-126, 182–188. http://treesearch.fs.fed.us/pubs/28418

Chorover, J., Troch, P. A., Rasmussen, C., Brooks, P. D., Pelletier, J. D., Breshears, D. D., Huxman, T.E., Kurc, S.A., Lohse, K. A., McIntosh, J.C., Meixner, T., Schaap, M.G., Litvak, M.E., Perdrial, J., Harpold, A., Durcik, M. (2011). How Water, Carbon, and Energy Drive Critical Zone Evolution: The Jemez-Santa Catalina Critical Zone

Observatory. Vadose Zone Journal, 10(3), 884–899. https://doi.org/10.2136/vzj2010.0132

Cole, K. (1983). Late Pleistocene vegetation of Kings Canyon, Sierra Nevada, California. Quaternary Research, 19(1), 117–129. https://doi.org/10.1016/0033-5894(83)90031-5

Corlett, R. T., & Westcott, D. A. (2013). Will plant movements keep up with climate change? Trends in Ecology and Evolution, 28(8), 482–488. https://doi.org/10.1016/j.tree.2013.04.003

Crawford, K.E., 1975, The geology of the Franciscan tectonic assemblage near Mount Hamilton, California (Ph.D. thesis): Los Angeles, University of California, 137p.

Cannon, J. B., Peterson, C. J., O'Brien, J. J., & Brewer, J. S. (2017). A review and classification of interactions between forest disturbance from wind and fire. *Forest Ecology and Management*, *406*(October), 381–390. https://doi.org/10.1016/j.foreco.2017.07.035

Daniels, M. L., Anderson, R. S., & Whitlock, C. (2005). Vegetation and fire history since the Late Pleistocene from the Trinity Mountains, northwestern California, USA. Holocene, 15(7), 1062–1071. https://doi.org/10.1191/0959683605hl878ra

Desta, F., Colbert, J. J., Rentch, J. S., & Gottschalk, K. W. (2004). Aspect induced differences in vegetation, soil, and microclimatic characteristics of an Appalachian watershed. Castanea, 69(2), 92–108.

Dibblee, T.W., Jr., and Minch, J.A., 2005, Geologic Map of the Diablo Quad- rangle, Contra Costa and Alameda Counties, California: Dibblee Geo- logical Foundation (Santa Barbara Museum of Natural History), Dibblee Foundation Map DF-162, scale 1:24,000.

Dixon, J., Heimsath, A., & Amundson, R. (2009). The critical role of climate and saprolite weathering in landscape evolution. Earth Surface Processes and Landforms, 34(June), 155–161. https://doi.org/10.1002/esp

Doane, T. H., Edmonds, D., Yanites, B. J., & Lewis, Q. (2021). Topographic Roughness on Forested Hillslopes: A Theoretical Approach for Quantifying Hillslope Sediment Flux From Tree Throw. Geophysical Research Letters, 48(20), 1–10. https://doi.org/10.1029/2021GL094987

Ernst, W. G. (2011). Accretion of the Franciscan Complex attending Jurassic-Cretaceous geotectonic development of northern and central California. *Bulletin of the Geological Society of America*, *123*(9–10), 1667–1678. https://doi.org/10.1130/B30398.1

Fan, Y., Clark, M., Lawrence, D. M., Swenson, S., Band, L. E., & Brantley, S. L. (2019). Hillslope hydrology in global change research and Earth system modeling. Water Resources Research, 55, 1737–1772. https://doi.org/10.1029/2018WR023903

Fan, Y., Grant, G., & Anderson, S. P. (2019). Water within, moving through, and shaping the Earth's surface: Introducing a special issue on water in the critical zone. Hydrological Processes, 3146–3151. https://doi.org/10.1002/hyp.13638

Ferdowsi, B., Gartner, J. D., Johnson, K. N., Kasprak, A., Miller, K. L., Nardin, W., Ortiz A.C., Tejedor, A. (2021). Earthcasting: Geomorphic Forecasts for Society. Earth's Future, 9(11), 1–24. https://doi.org/10.1029/2021EF002088

Flinchum, B. A., Holbrook, W. S., & Carr, B. J. (2022). What Do P-Wave Velocities Tell Us About the Critical Zone? Frontiers in Water, 3(January), 1–15. https://doi.org/10.3389/frwa.2021.772185

Flinchum, BA, Holbrook, WS, Grana, D, et al. Estimating the water holding capacity of the critical zone using near-surface geophysics. Hydrological Processes. 2018; 32: 3308– 3326. https://doi.org/10.1002/hyp.13260

Flinchum, B. A., Holbrook, W.S., Rempe, D., Moon, S., Riebe, C. S., Carr, B. J., Hayes J.L., St. Clair, J., Peters, M. P. (2018). Critical Zone Structure Under a Granite Ridge Inferred From Drilling and Three-Dimensional Seismic Refraction Data. Journal of

Geophysical Research: Earth Surface, 123(6), 1317–1343. https://doi.org/10.1029/2017JF004280

Gabet, E. J., Reichman, O. J., & Seabloom, E. W. (2003). The effects of bioturbation on soil processes and sediment transport. Annual Review Earth Planet. Sci, 31, 249–273. https://doi.org/10.1146/annurev.earth.31.100901.141314

Gabet, E. J., & Mudd, S. M. (2010). Bedrock erosion by root fracture and tree throw: A coupled biogeomorphic model to explore the humped soil production function and the persistence of hillslope soils. Journal of Geophysical Research: Earth Surface, 115(4), 1–14. https://doi.org/10.1029/2009JF001526

García-Gamero, V., Peña, A., Laguna, A. M., Giráldez, J. V, & Vanwalleghem, T. (2021). Factors controlling the asymmetry of soil moisture and vegetation dynamics in a hilly Mediterranean catchment. Journal of Hydrology, 598, 126207. https://doi.org/10.1016/j.jhydrol.2021.126207

Geldart, L. P., & Sheriff, R. E. (2004). Problems in exploration seismology and their solutions. Houston, TX: Society of Exploration Geophysicists.

Götmark, F., & Kiffer, C. (2014). Regeneration of oaks (Quercus robur/Q. petraea) and three other tree species during long-term succession after catastrophic disturbance (windthrow). Plant Ecology, 215(9), 1067–1080. https://doi.org/10.1007/s11258-014-0365-4

Gu, X., Mavko, G., Ma, L., Oakley, D., Accardo, N., Carr, B. J., Nyblade, A., Brantley, S. L. (2020). Seismic refraction tracks porosity generation and possible CO2 production at depth under a headwater catchment. Proceedings of the National Academy of Sciences of the United States of America, 117(32), 18991–18997. https://doi.org/10.1073/pnas.2003451117

Gutiérrez-Jurado, H. A., Vivoni, E. R., Cikoski, C., Harrison, B. J., Bras, R. L., & Istanbulluoglu, E. (2013). On the observed ecohydrologic dynamics of a semiarid basin with aspect-delimited ecosystems. *Water Resources Research*, *49*(12), 8263–8284. https://doi.org/10.1002/2013WR014364

Gutierrez-Jurado, H., Vivoni, E. R., Harrison, B. J., & Guan, H. (2006). Ecohydrology of root zone water fluxes and soil development in complex semiarid rangelands. *Hydrologic Processes*, *20*, 2267–2274. https://doi/10.1002/hyp.6333

Hahm, W. J., Rempe, D. M., Dralle, D. N., Dawson, T. E., Lovill, S. M., Bryk, A. B., Schieber, J., Dietrich, W. E. (2019). Lithologically Controlled Subsurface Critical Zone Thickness and Water Storage Capacity Determine Regional Plant Community Composition. Water Resources Research. https://doi.org/10.1029/2018WR023760

Hagedorn, F., Gavazov, K., & Alexander, J. M. (2019). Above- and belowground linkages shape responses of mountain vegetation to climate change. *Science*, *1123*(September), 1119–1123.

Hahm, W. J., Rempe, D. M., Dralle, D. N., Dawson, T. E., & Dietrich, W. E. (2020). Oak Transpiration Drawn From the Weathered Bedrock Vadose Zone in the Summer Dry Season. Water Resources Research, 56(11), 1–24. https://doi.org/10.1029/2020WR027419

Hahm, W. J., Dralle, D. N., Sanders, M., Bryk, A. B., Fauria, K. E., Huang, M. H., … Rempe, D. M. (2022). Bedrock Vadose Zone Storage Dynamics Under Extreme Drought: Consequences for Plant Water Availability, Recharge, and Runoff. Water Resources Research, 58(4), 1–23. https://doi.org/10.1029/2021WR031781

Hall, K. and Lamont, N. (2003) Zoogeomorphology in the Alpine: some observations on abiotic–biotic interactions, Geomorphology, 55, 219–234, https://doi.org/10.1016/S0169-555X(03)00141-7

Hasenmueller, E. A., Gu, X., Weitzman, J. N., Adams, T. S., Stinchcomb, G. E., Eissenstat, D. M., … Kaye, J. P. (2017). Weathering of rock to regolith: The activity of deep roots in bedrock fractures. Geoderma, 300, 11–31. https://doi.org/10.1016/j.geoderma.2017.03.020

Hayes, J. L., Riebe, C. S., Steven Holbrook, W., Flinchum, B. A., & Hartsough, P. C. (2019). Porosity production in weathered rock: Where volumetric strain dominates over chemical mass loss. *Science Advances*, *5*(9), 1–12. https://doi.org/10.1126/sciadv.aao0834

Heimsath, A. M., E. Dietrich, W., Nishiizumi, K., & Finkel, R. C. (1999). Cosmogenic nuclides, topography, and the spatial variation of soil depth. Geomorphology, 27(1–2), 151–172. https://doi.org/10.1016/S0169-555X(98)00095-6

Heusser, L. (1998). Direct correlation of millennial-scale changes in western North American vegetation and climate with changes in the California current system over the past ~60 kyr. Paleoceanography, 13(3), 252–262. https://doi.org/10.1029/98PA00670

Hinckley, E. L. S., Ebel, B. A., Barnes, R. T., Anderson, R. S., Williams, M. W., & Anderson, S. P. (2014). Aspect control of water movement on hillslopes near the rain-snow transition of the Colorado Front Range. Hydrological Processes, 28(1), 74–85. https://doi.org/10.1002/hyp.9549

Huang, M. H., Hudson-Rasmussen, B., Burdick, S., Lekic, V., Nelson, M. D., Fauria, K. E., & Schmerr, N. (2021). Bayesian Seismic Refraction Inversion for Critical Zone Science and Near-Surface Applications. Geochemistry, Geophysics, Geosystems, 22(5), 1–20. https://doi.org/10.1029/2020GC009172

Hughes, M. W., Almond, P. C., & Roering, J. J. (2009). Increased sediment transport via bioturbation at the last glacial-interglacial transition. Geology, 37(10), 919–922. https://doi.org/10.1130/G30159A.1

Inbar, A., Nyman, P., Rengers, F. K., Lane, P. N. J., & Sheridan, G. J. (2018). Climate Dictates Magnitude of Asymmetry in Soil Depth and Hillslope Gradient. Geophysical Research Letters, 45(13), 6514–6522. https://doi.org/10.1029/2018GL077629

Istanbulluoglu, E., Yetemen, O., Vivoni, E. R., Gutiérrez-Jurado, H. A., & Bras, R. L. (2008). Eco-geomorphic implications of hillslope aspect: Inferences from analysis of landscape morphology in central New Mexico. Geophysical Research Letters, 35(14), 1–6. https://doi.org/10.1029/2008GL034477

Ivory, S. J., Mcglue, M. M., Ellis, G. S., Lézine, A.-M., & Cohen, A. S. (2014). Vegetation Controls on Weathering Intensity during the Last Deglacial Transition in Southeast Africa. PLoS ONE, 9(11), 112855. https://doi.org/10.1371/journal.pone.0112855

Jackson, R.B., Schenk, H.J., Jobbágy, E.G., Canadell, J., Colello, G.D., Dickinson, R.E., Field, C.B., Friedlingstein, P., Heimann, M., Hibbard, K., Kicklighter, D.W., Kleidon, A., Neilson, R.P., Parton, W.J., Sala, O.E. and Sykes, M.T. (2000), Belowground Consequences of Vegetation Change and Their Treatment in Models. Ecological Applications, 10: 470-483. https://doi.org/10.1890/1051-0761(2000)010[0470:BCOVCA]2.0.CO;2

Kanso T, Gromaire MC, Ramier D, Dubois P, Chebbo G. An Investigation of the Accuracy of EC5 and 5TE Capacitance Sensors for Soil Moisture Monitoring in Urban Soils-Laboratory and Field Calibration. Sensors (Basel). 2020 Nov 14;20(22):6510. 10.3390/s20226510

Kulongoski, J. T., Hilton, D. R., Izbicki, J. A., & Belitz, K. (2009). Evidence for prolonged El Nino-like conditions in the Pacific during the Late Pleistocene: a 43 ka noble gas record from California groundwaters. Quaternary Science Reviews, 28(23–24), 2465–2473. https://doi.org/10.1016/j.quascirev.2009.05.008

Kumari, N., Saco, P. M., Rodriguez, J. F., Johnstone, S. A., Srivastava, A., Chun, K. P., & Yetemen, O. (2020). The Grass Is Not Always Greener on the Other Side: Seasonal Reversal of Vegetation Greenness in Aspect-Driven Semiarid Ecosystems. Geophysical Research Letters, 47(15), 1–12. https://doi.org/10.1029/2020GL088918

Langston, A. L., Tucker, G. E., Anderson, R. S., & Anderson, S. P. (2015). Evidence for climatic and hillslope-aspect controls on vadose zone hydrology and implications for saprolite weathering. Earth Surface Processes and Landforms, 40(9), 1254–1269. https://doi.org/10.1002/esp.3718

Lebedeva, M. I., & Brantley, S. L. (2013). Exploring geochemical controls on weathering and erosion of convex hillslopes: Beyond the empirical regolith production function. Earth Surface Processes and Landforms, 38(15), 1793–1807. https://doi.org/10.1002/esp.3424

Lebedeva, M. I., & Brantley, S. L. (2018). A clarification and extension of our model of regolith formation on hillslopes. Earth Surface Processes and Landforms, 43(13), 2715–2723. https://doi.org/10.1002/esp.4426

Lebedeva, M. I., & Brantley, S. L. (2020). Relating the depth of the water table to the depth of weathering. *Earth Surface Processes and Landforms*, *45*(9), 2167–2178. https://doi.org/10.1002/esp.4873

Lucas, Y. (2001). The role of plants in controlling rates and products of weathering: Importance of biological pumping. Annual Review of Earth and Planetary Sciences, 29(May 2001), 135–163. https://doi.org/10.1146/annurev.earth.29.1.135

Ma, L., Oakley, D., Nyblade, A., Moon, S., Accardo, N., Wang, W., et al. (2021). Seismic imaging of a shale landscape under compression shows limited influence of topography-induced fracturing. Geophysical Research Letters, 48, e2021GL093372. https://doi.org/10.1029/2021GL093372

Maher, K., & Navarre-Sitchler, A. (2019). Reactive Transport Processes that Drive Chemical Weathering: From Making Space for Water to Dismantling Continents. *Reviews in Mineralogy and Geochemistry*, *85*(1), 349–380. https://doi.org/10.2138/rmg.2018.85.12

Marshall, H. P., Chandler, D. G., Benner, S. G., & Mcnamara, J. P. (2011). Aspect influences on soil water retention and storage. Hydrological Processes, 25(25), 3836–3842. https://doi.org/10.1002/hyp.8281

Maxwell, A. E., & Shobe, C. M. (2022). Land-surface parameters for spatial predictive mapping and modeling. Earth-Science Reviews, 226(September 2021), 103944. https://doi.org/10.1016/j.earscirev.2022.103944

McGuire, L. A., Pelletier, J. D., & Roering, J. J. (2014). Development of topographic asymmetry: Insights from dated cinder cones in the western United States. Journal of Geophysical Research F: Earth Surface, 119(8), 1725–1750. https://doi.org/10.1002/2014JF003081

McKnight, P., & Najab, J. (2010). Mann-Whitney U Test. Dictionary of Statistics & Methodology, 2009. https://doi.org/10.4135/9781412983907.n1115

Mensing, S. (2005). The history of oak woodlands in California, part I: the paleoecologic record.

Metropolis, N., Rosenbluth, A. W., Rosenbluth, M. N., Teller, A. H., & Teller, E. (1953). Equation of state calculations by fast computing machines. The Journal of Chemical Physics, 21, 1087–1092. https://doi.org/10.1063/1.1699114

Montgomery, D. R. (1993). Compressional uplift in the central California Coast Ranges. *Geology*, *21*(6), 543–546. https://doi.org/10.1130/0091-7613(1993)021<0543:CUITCC>2.3.CO;2

Moon, S., Perron, J. T., Martel, S. J., Holbrook, W. S., and St. Clair, J. (2017), A model of three-dimensional topographic stresses with implications for bedrock fractures, surface processes, and landscape evolution, J. Geophys. Res. Earth Surf., 122, 823–846, doi:10.1002/2016JF00415.

Nielson, T., Bradford, J., Holbrook, W. S., & Seyfried, M. (2021). The Effect of Aspect and Elevation on Critical Zone Architecture in the Reynolds Creek Critical Zone Observatory: A Seismic Refraction Study. Frontiers in Water | Www.Frontiersin.Org, 1, 670524. https://doi.org/10.3389/frwa.2021.670524

Nimmo, J. R. (2012). Preferential flow occurs in unsaturated conditions. Hydrological Processes, 26(5), 786–789.

Nimmo, J. R. (2021). The processes of preferential flow in the unsaturated zone. Soil Science Society of America Journal, 85(1), 1–27. https://doi.org/10.1002/saj2.20143

Page, B. M. (1999). Geology of the lick observatory quadrangle, california. International Geology Review, 41(4), 355–367. https://doi.org/10.1080/00206819909465146

Pawlik, Ł., Phillips, J. D., & Šamonil, P. (2016). Roots, rock, and regolith: Biomechanical and biochemical weathering by trees and its impact on hillslopes-A critical literature review. Earth-Science Reviews, 159, 142–159. https://doi.org/10.1016/j.earscirev.2016.06.002

Pedrazas, M. A., Hahm, W. J., Huang, M.-H., Dralle, D., Nelson, M. D., Breunig, R. E., et al. (2021). The relationship between topography, bedrock weathering, and water storage across a sequence of ridges and valleys. Journal of Geophysical Research: Earth Surface, 126, e2020JF005848. https://doi.org/10.1029/2020JF005848

Pelletier, J. D., Barron-Gafford, G. A., Gutiérrez-Jurado, H., Hinckley, E.-L. S., Istanbulluoglu, E., McGuire, L. A., Niu, G.-Y., Poulos, M. J., Rasmussen, C., Richardson, P., Swetnam, T. L., and Tucker, G. E. (2018) Which way do you lean? Using slope aspect variations to understand Critical Zone processes and feedbacks. Earth Surf. Process. Landforms, 43: 1133– 1154. doi: 10.1002/esp.4306.

Perron, J. T. (2017). Climate and the Pace of Erosional Landscape Evolution. Annual Review of Earth and Planetary Sciences, 45(August), 1–71.

Poulos, M. J., Pierce, J. L., Flores, A. N., & Benner, S. G. (2012). Hillslope asymmetry maps reveal widespread, multi-scale organization. Geophys. Res. Lett, 39, 6406. https://doi.org/10.1029/2012GL051283

Raymond, L. A. (2014). Designating tectonostratigraphic terranes versus mapping rock units in subduction complexes: Perspectives from the Franciscan Complex of California, USA. International Geology Review, 57(5–8), 801–823. https://doi.org/10.1080/00206814.2014.911124

Raymond, L. A. (2018). What is Franciscan?: revisited. International Geology Review, 60(16), 1968–2030. https://doi.org/10.1080/00206814.2017.1396933

Regmi, N. R., McDonald, E. V, & Rasmussen, C. (2019). Hillslope response under variable microclimate. Earth Surface Processes and Landforms, 44(13), 2615–2627. https://doi.org/https://doi.org/10.1002/esp.4686

Rempe, D. M., & Dietrich, W. E. (2014). A bottom-up control on fresh-bedrock topography under landscapes. Proceedings of the National Academy of Sciences, 111(18), 6576–6581. https://doi.org/10.1073/pnas.1404763111

Rempe, D. M., & Dietrich, W. E. (2018). Direct observations of rock moisture, a hidden component of the hydrologic cycle. Canadian Journal for Resources, 26(1346–1352). https://doi.org/10.1073/pnas.1800141115

Riebe, C. S., Kirchner, J. W., Granger, D. E., & Finkel, R. C. (2001). Strong tectonic and weak climatic control of long-term chemical weathering rates. Geology, 29(6), 511–514. https://doi.org/10.1130/0091-7613(2001)029

Roering, J.J., Almond, P., McKean, J., and Tonkin, P., 2002, Soil transport driven by biological processes over millennial timescales: Geology, v. 30, p. 1115–1118, doi: 10.1130/0091-7613(2002)030<1115:STDBBP >2.0.CO;2.

Sharp, R. P. (1982). Landscape evolution (A Review). Proceedings of the National Academy of Sciences, 79(14), 4477–4486. https://doi.org/10.1073/pnas.79.14.4477

Smith, T., & Bookhagen, B. (2020). Climatic and Biotic Controls on Topographic Asymmetry at the Global Scale. https://doi.org/10.1029/2020JF005692

Sólyom, P. B. (2004). Effect of limited storm duration on landscape evolution, drainage basin geometry, and hydrograph shapes. *Journal of Geophysical Research*, *109*(F3), 1–13. https://doi.org/10.1029/2003jf000032

St. Clair, J., Moon, S., Holbrook, W. S., Perron, J. T., Riebe, C. S., Martel, S. J., Carr B., Harman C., Richter, D. B. (2015). Geophysical imaging reveals topographic stress control of bedrock weathering. Science, 350(6260), 534–538. https://doi.org/10.1126/science.aab2210

Szwagrzyk, J., Gazda, A., Dobrowolska, D., Chećko, E., Zaremba, J., & Tomski, A. (2018). Natural regeneration following wind disturbance increases the diversity of managed lowland forests in NE Poland. Journal of Vegetation Science, 29(5), 898–906. https://doi.org/10.1111/jvs.12672

Tang, Q., Duncan, J. M., Guo, L., Lin, H., Xiao, D., & Eissenstat, D. M. (2020). On the controls of preferential flow in soils of different hillslope position and lithological origin. Hydrological Processes. https://doi.org/10.1002/hyp.13883

Tague N., (2022) Plants rooted in rocks. Nat. Geosci. https://doi.org/10.1038/s41561-022-01030-0

Übernickel, K., Pizarro-Araya, J., Bhagavathula, S., Paulino, L., & Ehlers, T. A. (2021). Reviews and syntheses: Composition and characteristics of burrowing animals along a climate and ecological gradient, Chile. Biogeosciences, 18(20), 5573–5594. https://doi.org/10.5194/bg-18-5573-2021

U.S. Geological Survey 3D Elevation Program (2020). Santa Clara County, CA Lidar. Distributed by OpenTopography. https://portal.opentopography.org/usgsDataset?dsid=CA_SantaClaraCounty_2020. Accessed: 2021-01-21.

Wang, W., Chen, P., Dueker, K., Zhang, Y., Lee, E.-j., Mu, D., et al. (2021). Coevolution of weathering front and water table. Geophysical Research Letters, 48, e2021GL092916. https://doi.org/10.1029/2021GL092916

West, N., Kirby, E., Nyblade, A. A., & Brantley, S. L. (2019). Climate preconditions the Critical Zone: Elucidating the role of subsurface fractures in the evolution of asymmetric topography. Earth and Planetary Science Letters, 513, 197–205. https://doi.org/10.1016/j.epsl.2019.01.039

Wentworth, C. M., Blake, M. C., Mclaughlin, R. J., & Graymer, R. W. (1999). Preliminary geologic description of the San Jose 30 X 60 minute quadrangle, California. Open-File Report 98-795, 1–52.

Yetemen, O., Istanbulluoglu, E., Homero Flores-Cervantes, J., Vivoni, E., & Bras, R. (2015). Ecohydrologic role of solar radiation on landscape evolution, 1127–1157. https://doi.org/10.1002/2014WR016169

Zapata-Rios, X., Brooks, P. D., Troch, P. A., McIntosh, J., and Guo, Q. (2016) Influence of terrain aspect on water partitioning, vegetation structure and vegetation greening in high-elevation catchments in northern New Mexico. Ecohydrol., 9: 782– 795. doi: 10.1002/eco.1674.